

Investigating the Surface Properties and Evolution of a Desert Playa Using Optical and Radar Satellite Imagery Products

Iyasu Eibedingil¹, Daniel Tong², and Thomas Gill¹

¹University of Texas at El Paso

²George Mason University Foundation Inc.

November 22, 2022

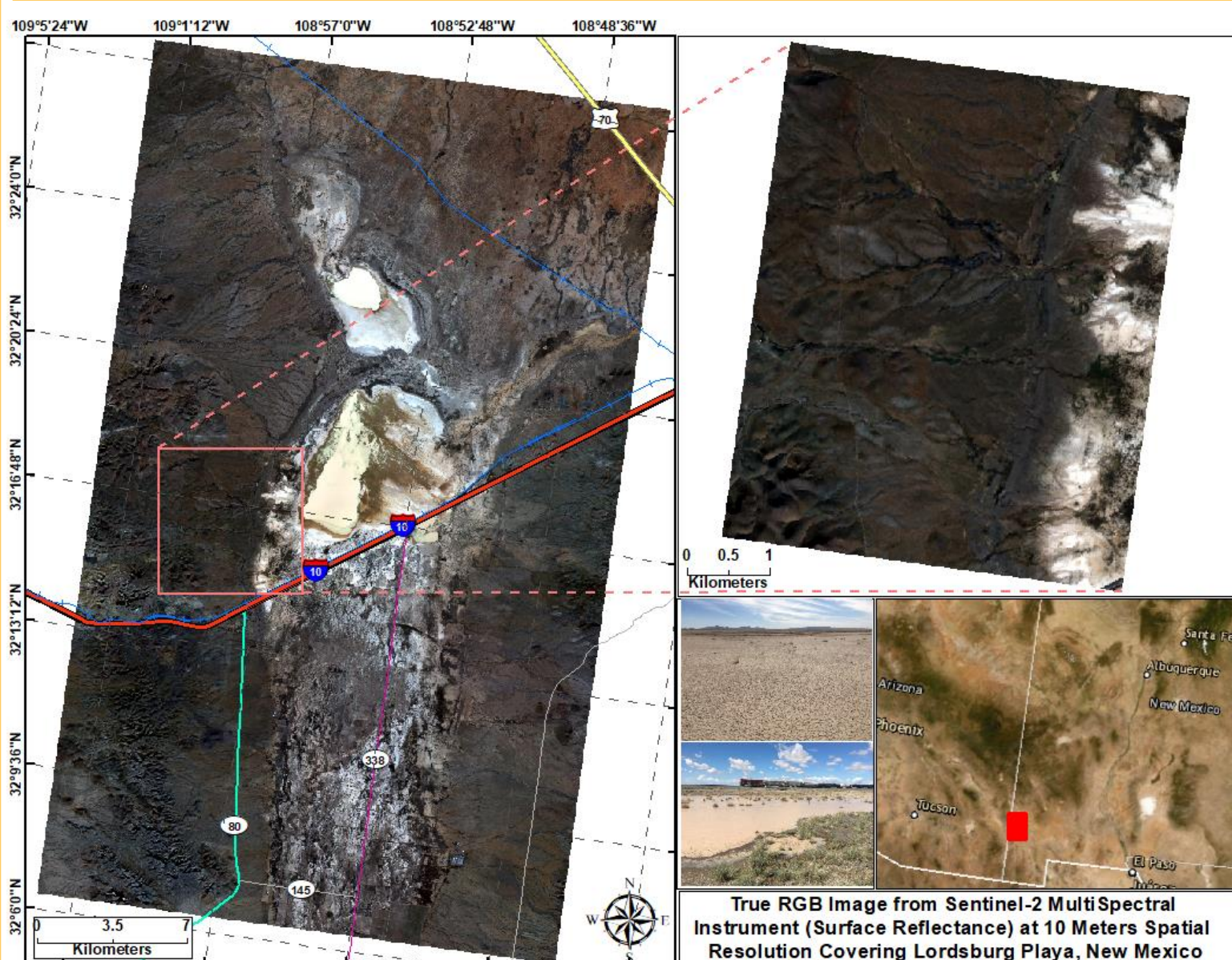
Abstract

In connection to drought, the southwestern United States is experiencing an increase in blowing dust, an increase in incidence of valley fever, an increase in visibility-related traffic accidents, reduction in solar panel efficiency, and earlier mountain snowmelt. The response of the land surface to the wind is greatly dependent on the proportion of land cover, soil and sediment characteristics, weather conditions, and spatial distribution of vegetation, all factors affecting aeolian processes. Combined use of optical and radar satellite imagery products can provide invaluable benefits in characterizing surface properties of desert playas (ephemeral lakes)- the preferred landform for wind erosion. As a home for high temporal coverage of Landsat optical images and a cloud computing platform, Google Earth Engine (GEE) provides a multi-petabyte catalog of satellite imagery, powerful algorithms, and application programming interface capabilities. Processing and analyzing moderate to high spatial resolution images from Landsat and Sentinel-2 in GEE are crucial resources for extracting contributions of different endmembers to pixel mixtures. Radar images, with the capability to penetrate through clouds, darkness, and rain, have a power to detect the extent and levels of changes in land cover and soil moisture. In this study, we identified the fractional abundance of soil, vegetation, and water endmembers of each pixel of images using the spectral unmixing algorithm in GEE in Lordsburg Playa (New Mexico, USA), which is prone to aeolian erosion. Here, we used Landsat-8 and Landsat-5 at 30 meters spatial resolution and Sentinel-2 Multispectral instrument at 10-20 meters resolution. By employing Interferometric Synthetic Aperture Radar (InSAR) techniques, we explored the changes in the water level of the playa and the possible hot spots of erosion-inducing sediment loading to the playa. In this data recipe, we analyzed a pair of Sentinel-1 images that bracket a monsoon day with high rainfall event and a pair of images representing dry day and monsoon day. The results from this approach clearly show locations prone to the change in phase and displacement due to water and thus sediment loading susceptible to wind.

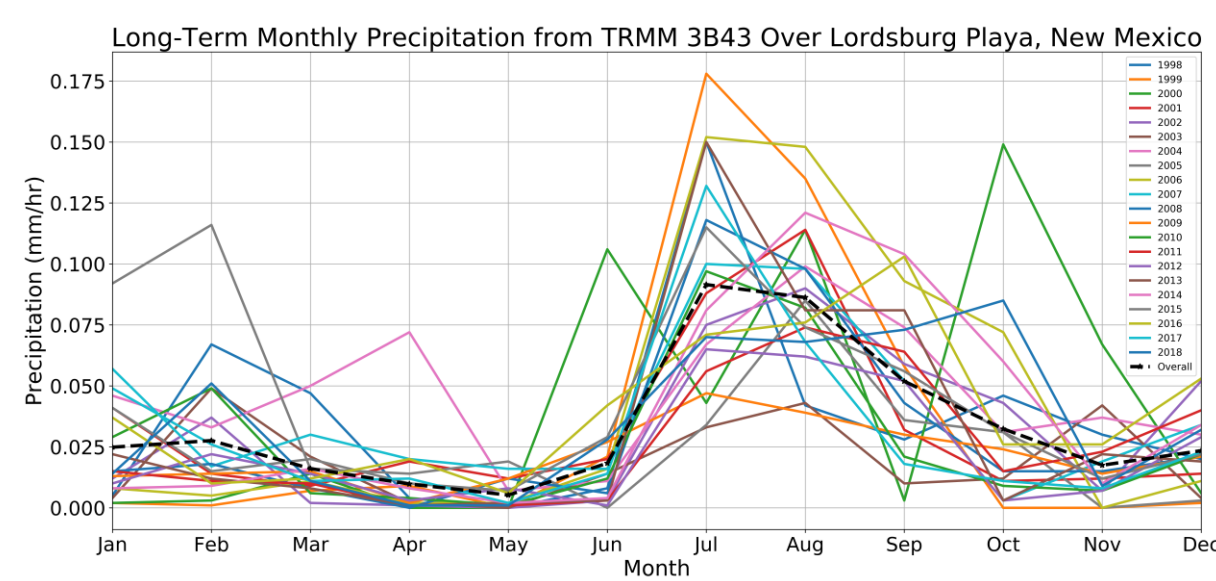
ABSTRACT

In connection to drought, the southwestern United States is experiencing an increase in blowing dust, an increase in incidence of valley fever, an increase in visibility-related traffic accidents, reduction in solar panel efficiency, and earlier mountain snowmelt. The response of the land surface to the wind is greatly dependent on the proportion of land cover, soil, and sediment characteristics, weather conditions, and spatial distribution of vegetation, all factors affecting aeolian processes. By utilizing spectral unmixing algorithm on the optical imagery products of Landsat and Sentinel-2, we identified the fractional abundance of soil, vegetation, and water endmembers of each pixel of the images in the Lordsburg Playa, New Mexico. The algorithm performed very well in estimating the abundance of the endmembers. In addition, by employing Interferometric Synthetic Aperture Radar (InSAR) techniques on a pair of Sentinel-1 radar images, we investigated the water level changes in the Lordsburg Playa and possible hot spots of erosion-inducing sediment loading to the playa. The results from this approach clearly show locations prone to the change in phase and displacement due to water level change and thus sediment loading susceptible to wind.

1. SITE DESCRIPTION: LORDSBURG PLAYA, NEW MEXICO



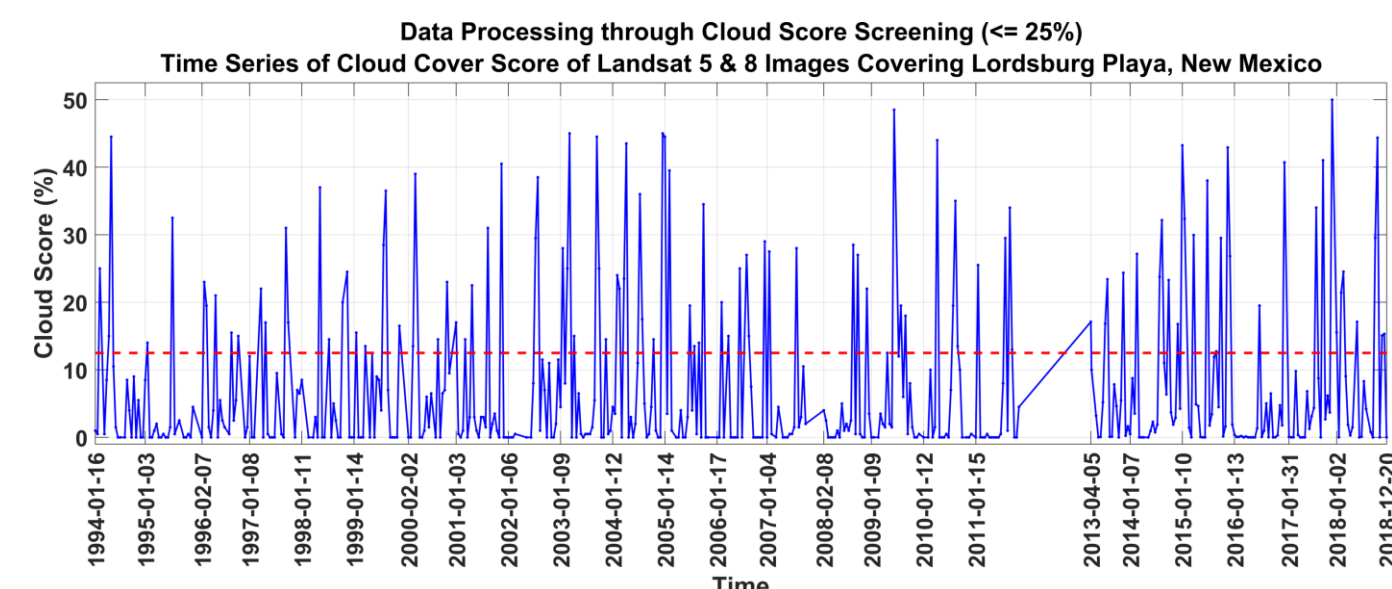
- Inundation by highly variable seasonal rainfall (mostly summer).
- Sediment loading through runoff erosion and berm bursting.
- Deposition of sand, silt, and clay sediments on to playa.
- Crust formation (salts) as a result of evaporation.
- An increase on the availability of loose surface sediments through anthropogenic disturbance, facilitating aeolian saltation process.
- One of the sources of the most intense dust storms in the Chihuahuan Desert. Hazard on highway I-10 crossing the playa.



2. DATA & METHODS

2.1. Data

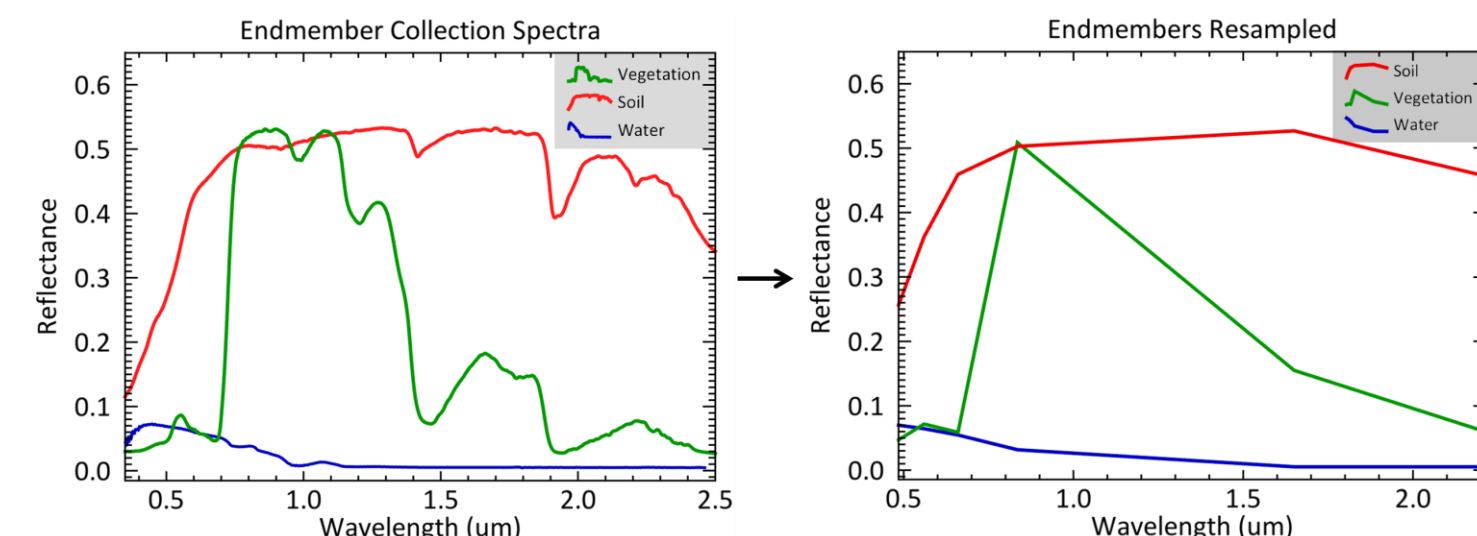
- **USGS: Landsat 5 & 8 Surface Reflectance Tier 1**
 Spatial resolution: 30 meters
 Temporal coverage: Landsat 5 from Jan. 1994 to May 2012
 Landsat 8 from Apr. 2013 to Dec. 2018
- **European Space Agency: Sentinel-2 Multispectral instrument**
 Spatial resolution: 10 – 60 meters
 Temporal coverage: Jan. 2016 to Dec. 2018.



- **USGS: Spectral Library Version 7, spectral signatures of water, soil, & vegetation**
- **European Space Agency: Sentinel-1 C – band Synthetic Aperture Radar Ground Range Detected**
 Pair of images (from 24 Jul. & 5 Aug. 2017) that bracket a very wet monsoon day of 1 Aug. 2017 with relatively highest rainfall event & another pair of images representing dry day (14 Mar. 2017) and wet day (5 Aug. 2017).

2.2. Methods

- **Spectral Resampling** (convolved from Analytical Spectral Devices (ASD) to Landsat 5 spectral resolution, Landsat 8 already resampled)



- **Linear Spectral Unmixing, Water Flagging, & Edge Detection**

$$\sum_{\lambda=1}^7 Y_{i\lambda} = \sum_{\lambda=1}^7 \beta_{11} V_{\lambda} + \sum_{\lambda=1}^7 \beta_{12} S_{\lambda} + \sum_{\lambda=1}^7 \beta_{13} W_{\lambda} + \sum_{\lambda=1}^7 \epsilon_{i\lambda}$$

$$\begin{bmatrix} Y_{i1} \\ Y_{i2} \\ \vdots \\ Y_{i7} \end{bmatrix} = \begin{bmatrix} V_1 & S_1 & W_1 \\ V_2 & S_2 & W_2 \\ \vdots & \vdots & \vdots \\ V_7 & S_7 & W_7 \end{bmatrix} \begin{bmatrix} \beta_{11} \\ \beta_{12} \\ \beta_{13} \end{bmatrix} + \begin{bmatrix} \epsilon_{i1} \\ \epsilon_{i2} \\ \vdots \\ \epsilon_{i7} \end{bmatrix}$$

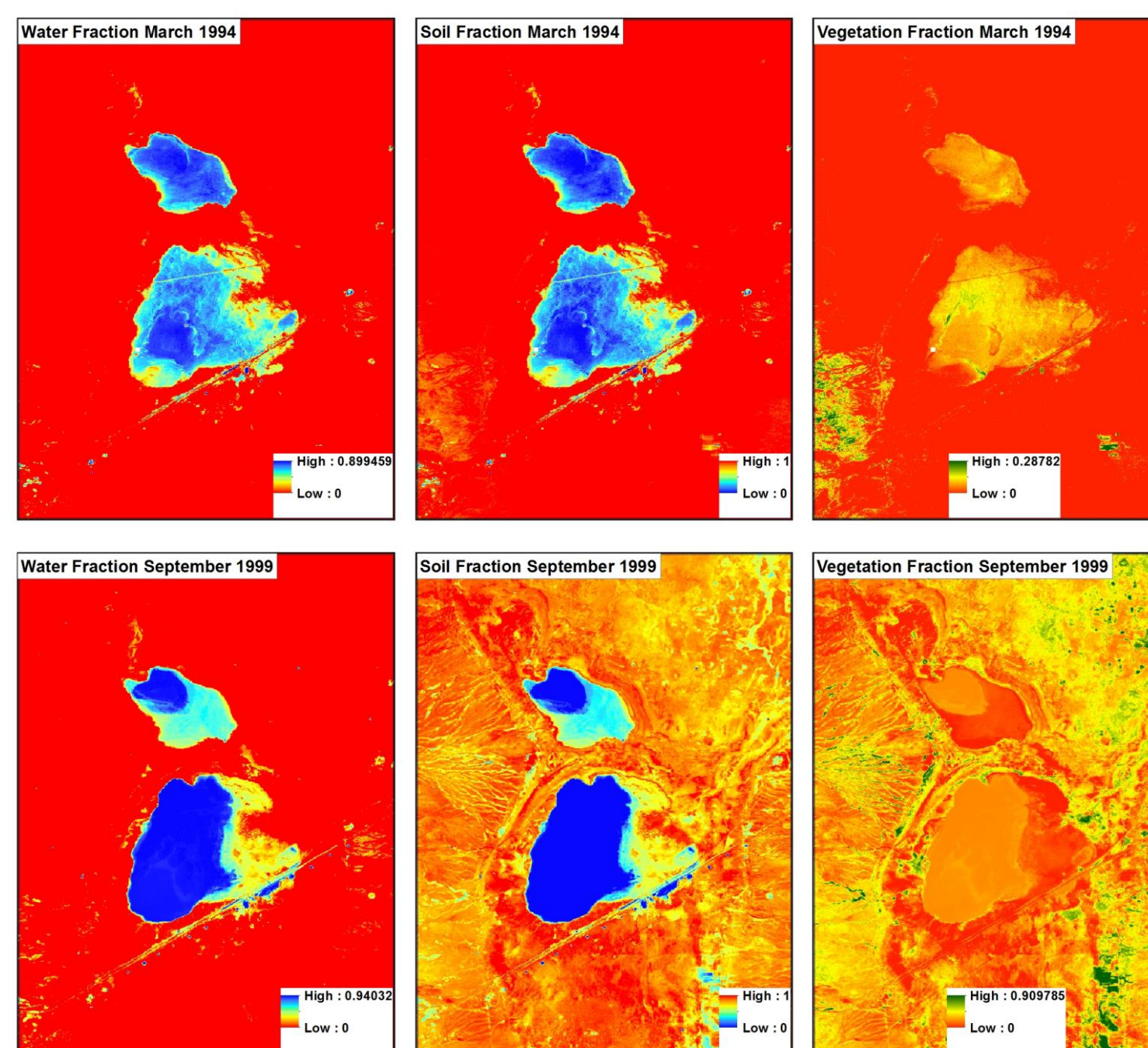
Known terms $Y = M * \beta + \epsilon$ Fractions to be determined

Constrains
 $\beta_1 + \beta_2 + \beta_3 = 1$
 $\beta_1 \geq 0, \beta_2 \geq 0, \text{ and } \beta_3 \geq 0$

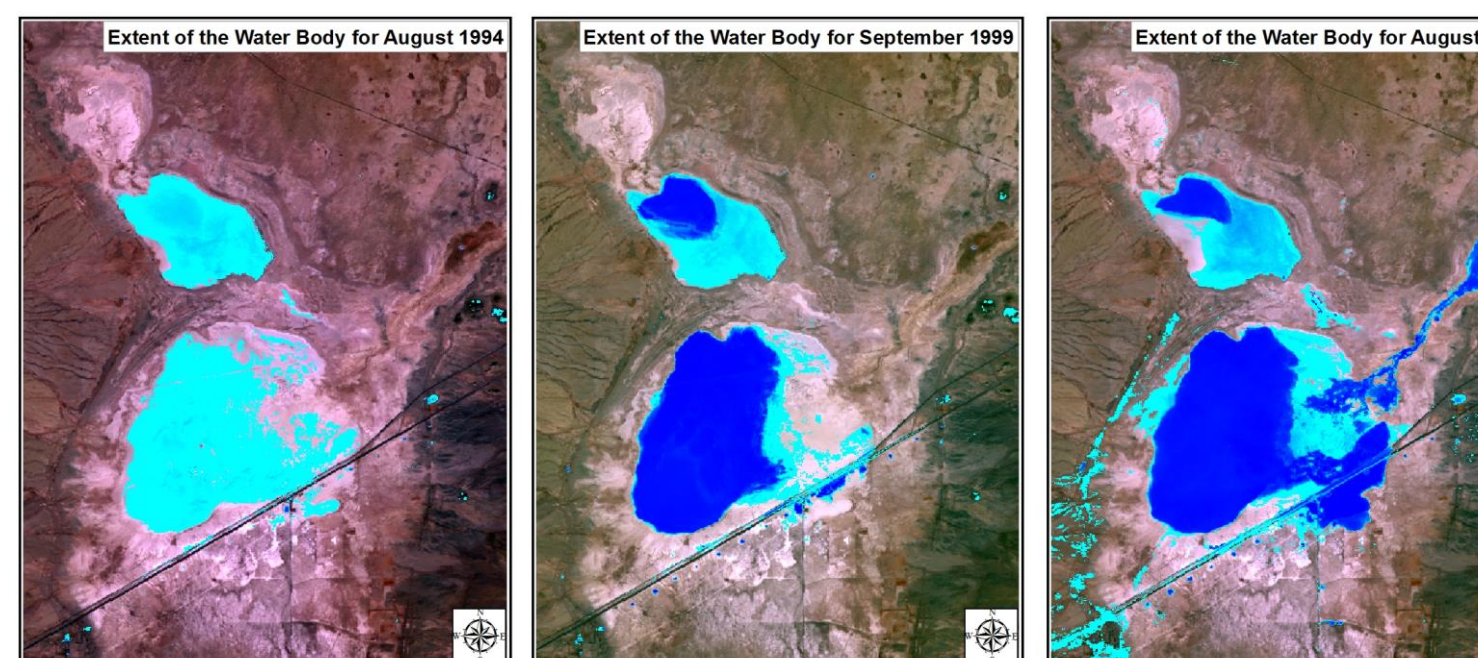
- **Deformation Estimation** (interferometric SAR phase processing using Sentinel Application Platform (SNAP) tool and displacement analysis through interferometric phase unwrapping in SNAPHU which is a two-dimensional phase unwrapping algorithm)

3. RESULTS & DISCUSSION

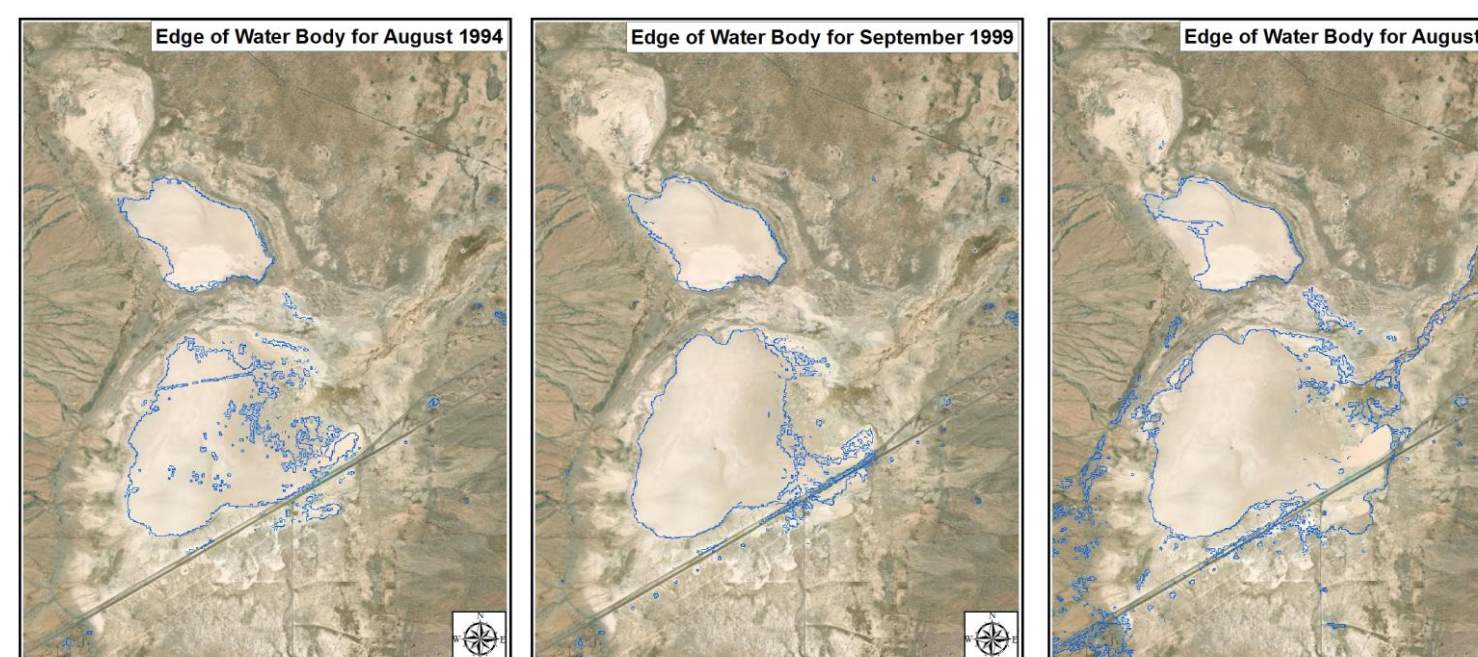
3.1. Linear Spectral Unmixing (Fraction of Endmembers)



3.2. Water Pixel Flagging (0.35 as a threshold)



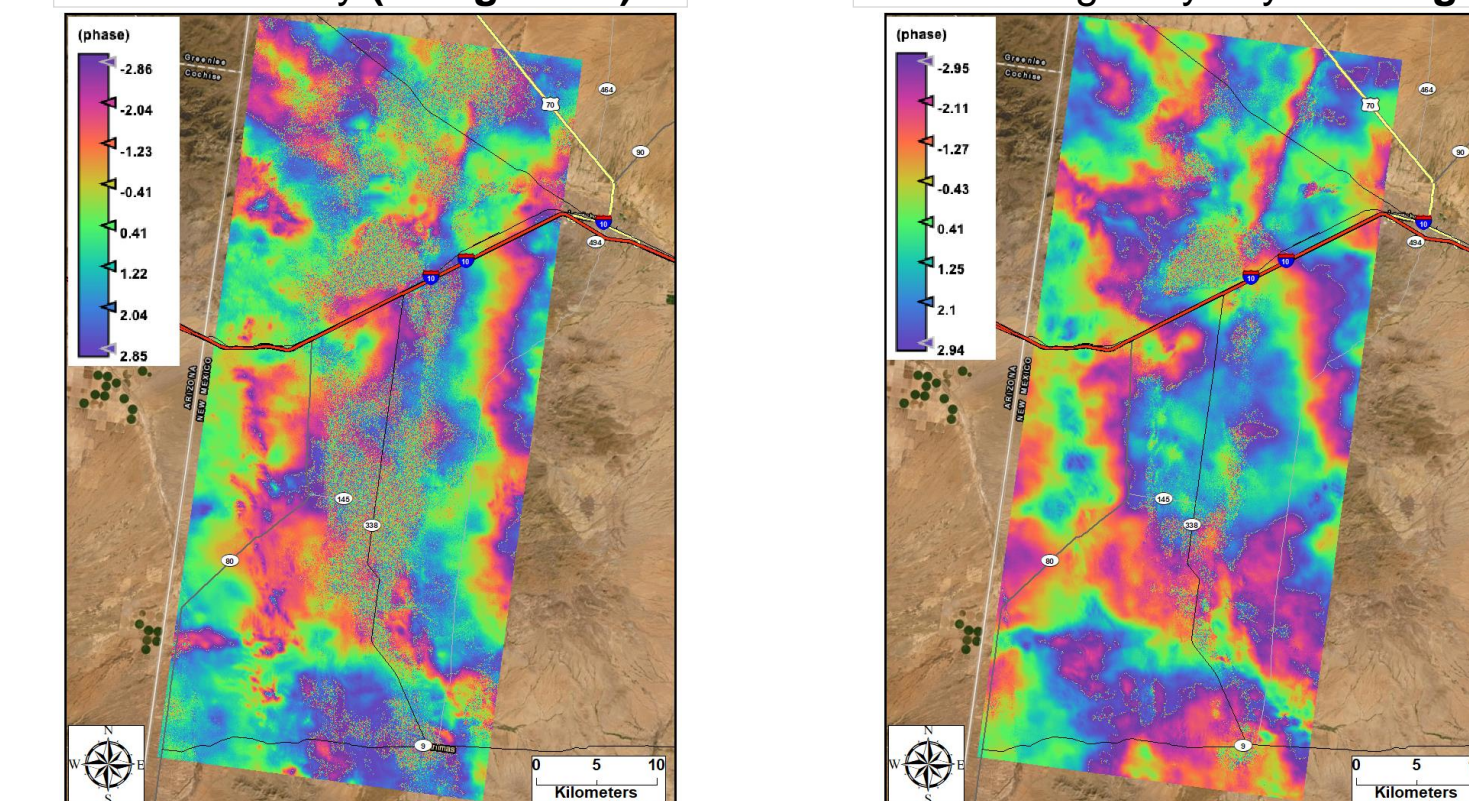
3.3. Edge Detection



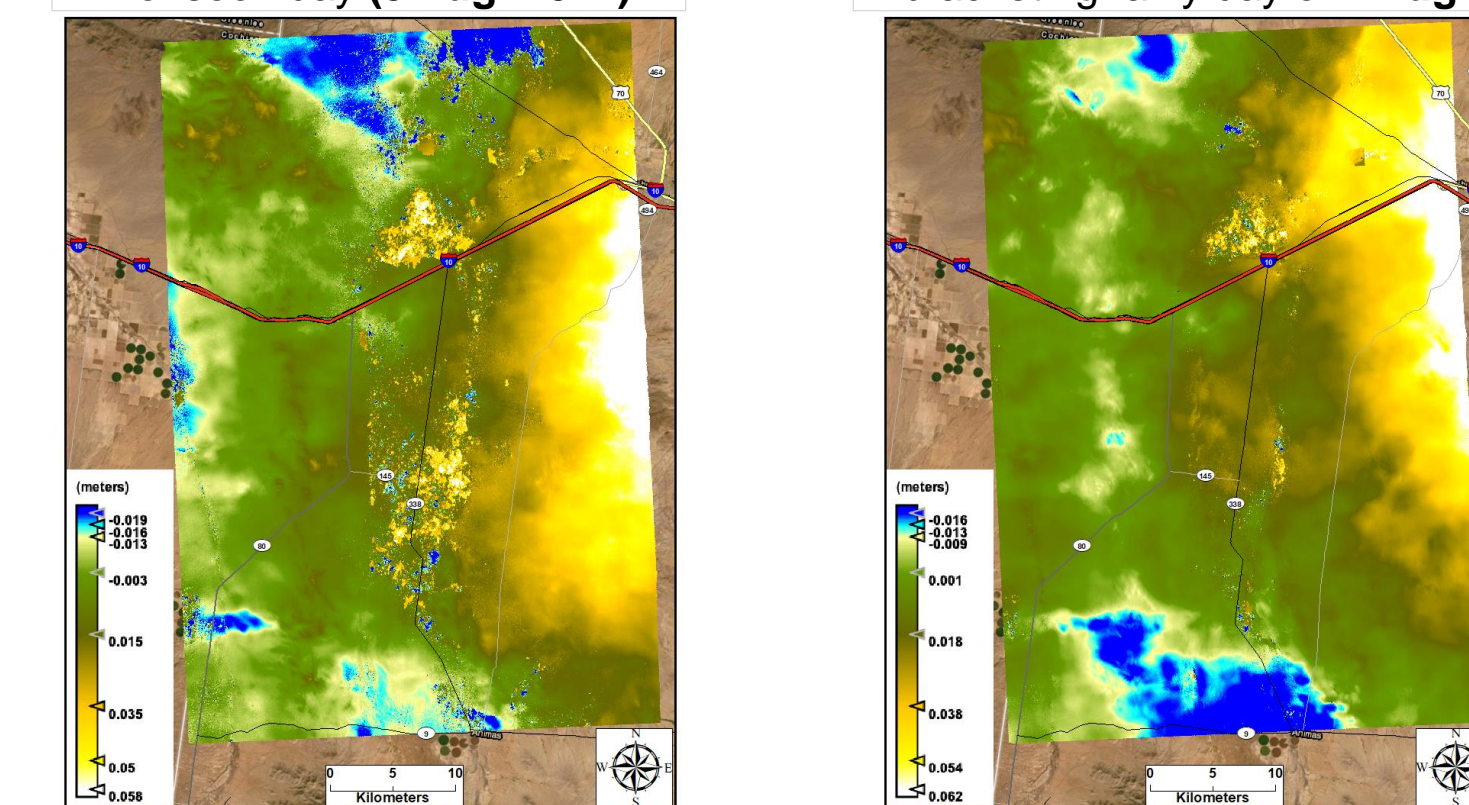
- The linear spectral unmixing algorithm performed very well in estimating the fraction of endmembers over the Lordsburg Playa.
- The results from Sentinel-2 were superior as most of the Sentinel-2 bands have finer spatial and spectral resolution than Landsat bands.

3.4. Deformation Investigation

- **Deformation fringes from interferogram phase analysis between:**
 Spring day (14 Mar. 2017) & monsoon day (5 Aug. 2017) 24 Jul. 2017 & 5 Aug. 2017 bracketing rainy day of 1 Aug.



- **Displacement maps between:**
 Spring day (14 Mar. 2017) & monsoon day (5 Aug. 2017) 24 Jul. 2017 & 5 Aug. 2017 bracketing rainy day of 1 Aug.



4. SUMMARY AND CONCLUSIONS

- The surface deformations identified between the pair images were mainly due to the seasonal rainfall and sediment loading transported by runoff.
- The movement of the edge of the water body in the playa from wet to dry season and vice versa, increases the availability of the sediments for wind erosion along the edge of the water body.
- The results from radar image analysis clearly showed locations prone to the change in phase and displacement due to water level change and thus sediment loading susceptible to wind.
- The combination of optical and radar satellite images improved the mapping of hotspots of wind erosion prone regions.

REFERENCES

[1] Gorelick, N., Hancher, M., Dixon, M., Ilyushchenko, S., Thau, D., & Moore, R. (2017). Google Earth Engine: Planetary-scale geospatial analysis for everyone. *Remote Sensing of Environment* 202:18-27.
 [2] Copernicus Sentinel data 2017. Retrieved from ASF DAAC 2019, processed by ESA.

ACKNOWLEDGMENTS

We acknowledge the funding support of USDOT CARTEEH project UTEP-01-13, NASA grants 80NSSC19K0195 and NNX16AH13G, and travel grants from the UTEP Graduate School and UTEP Student Government Association.